PERIODICA POLYTECHNICA SER. EL. ENG. VOL. 37, NO. 4, PP. 327-336 (1993)

STARTING TORQUE OF THE INDUCTION MACHINE WITH STARTING DISC

Gyula TŐKE and Sándor JANKA

Department of Electrical Machines
Technical University of Budapest
H-1521 Budapest, Hungary

Received: April 13, 1993

Abstract

As it is well known, with the increase of the unit output, the relative starting torque (related to the nominal value) decreases in the induction machine with squirrel-cage rotor. This effect can be partially eliminated by using a new type patented rotor, having a starting disc. The disc, made of *ferromagnetic material*, is fixed to the shaft near the end rings of the single-cage basic machine. The discs can be regarded as a solid rotor where the stator is formed by the end windings of the basic machine. A further effect is that it causes skin effect in the neighbouring end rings (resistance increase in the rotor circuit of the basic machine). The increase of the starting torque is proportional to the sum of the eddy-current losses in the starting discs and the surplus loss in the end rings. The rotor, with starting discs, can be used with the best results for induction machines of high output and small pole number ($P_n > 500$ kW, $p \leq 2$).

Keywords: induction machine with starting disc, starting torque.

Introduction

As it is well known, with the increase of the unit output, the relative starting torque (related to the nominal value) decreases in the induction machine with squirrel-cage rotor. This effect can be partially eliminated by using a new type patented rotor, having a starting disc. The disc, made of *ferromagnetic material* is fixed to the shaft near the end rings of the single-cage basic machine (*Fig. 1*). The discs can be regarded as a solid rotor where the stator is formed by the end windings of the basic machine. A further effect is that it causes skin effect in the neighbouring end rings (resistance increase in the rotor circuit of the basic machine). The increase of the starting torque is proportional to the sum of the eddy-current losses in the starting discs and the surplus loss in the end rings. The rotor, with starting discs, can be used with the best results for induction machines of high output and small pole number ($P_n > 500$ kW, $p \leq 2$).

The above mentioned loss components can be controlled by the linear dimensions and by the distance between the starting disc and the ring.

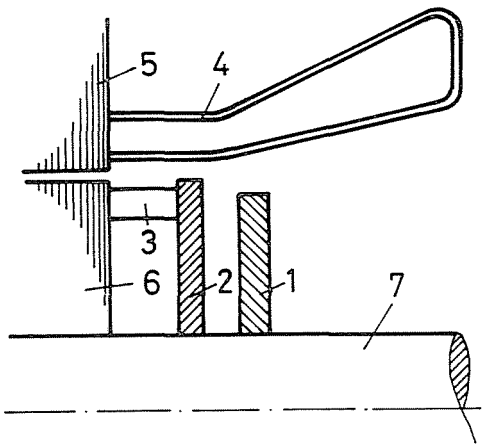

Fig. 1. Induction motor with rotor having a starting disc
1. Starting disk
2. End ring
3. Rotor bars
4. Stator end winding
5. Stator core 6. Rotor core 7. Shaft

For test purposes Ganz Ansaldo Ltd. produced an end winding model in 1:1 size of a two-pole induction motor — with single-cage and fixed rotor — for the 1000 kW/1600 kW types (disregarding the axial size of the lamination). With the help of this model measurement series were carried out with starting disc of different sizes.

Hereunder we outline the results achieved during the measurement series carried out for the loss components. Concerning the effect of the starting disc on the end winding flux of the machine we refer to the paper [1].

Loss at the End Ring

The loss at the end ring with specific resistance ρ_g and volume V_g can be calculated in knowledge of the current density distribution (J_g):

$$P_g = \rho_g \cdot \int\limits_{(V_g)} J_g^2 \cdot dV_g.$$

The end ring can be regarded as a disc type conductor.

Its current density considerably varies in function of the radius (r) and the distance between the ring and the starting disc (t) (*Fig. 2*). The

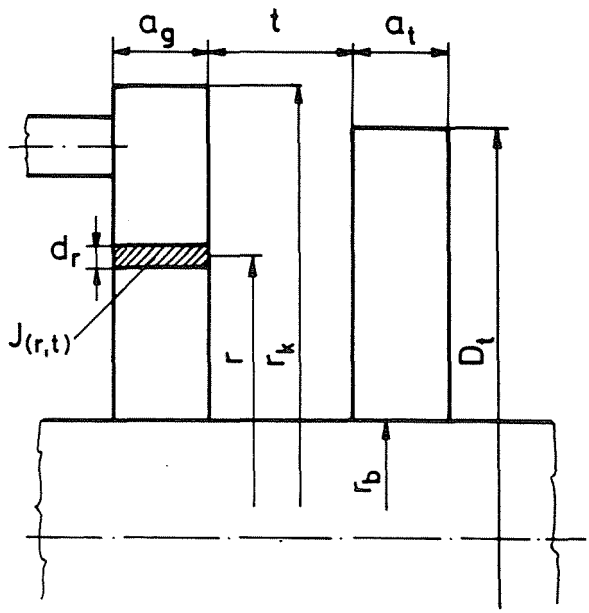

Fig. 2. Markings of the end ring and the starting dimensions

volume element of a ring with a_g thickness is as follows:

$$dV_g = 2\pi a_g \cdot r \cdot dr.$$

With the help of the above, in function of distance 't', the loss is the following:

$$P_g(t) = 2\pi \cdot a_g \cdot \rho_g \cdot \int_{r_b}^{r_b} J_g^2(r,t) r \cdot dr.$$

As a basis of comparison let us choose the loss corresponding to the ring without current displacement:

$$P_{go} = \rho_g \cdot J_K^2 \cdot V_g.$$

Here J_K means the current density value calculated with the current (I_g), and the cross-section (A_g) of the ring:

$$J_K = I_g / A_g.$$

Let us introduce the local current density related to the mean value:

$$j(r,t) = J(r,t)/J_K$$

as well as the mean radius and the height of the ring as follows:

$$R_K = (r_b + r_k)/2, \qquad H = r_K - r_b.$$

The relative loss value is the following:

$$p_g(t) = P_g(t)/P_{go} = \frac{1}{R_K H} \cdot \int_{r_b}^{r_b} j^2(r,t) r \cdot dr.$$

For determining the current density distribution, references [2,3,4] provide several approximate calculation methods. However, only a few papers discuss experimental verification of the calculation results. The measurement method developed by us and applied to the end winding model is based on the Rogowsky coil. As it is well known, thevoltage (U) induced in the Rogowsky coil is proportional to the current of the sourrounding conductor and to the angular frequency. The effective current value of calibration angular frequency can be determined by measuring the induced voltage of the coil with C_R constant

$$I = C_R \cdot U.$$

For measuring the current distribution the 'A' section of the conductor is divided into partial cross-sections $A_1, A_2, \ldots A_n$ with the help of small orifices, those do not disturb the electric conduction significantly, then $I_1, I_2, \ldots I_n$ currents are measured with the help of a Rogowsky coil (*Fig. 3*). The mean current density value of the i-th cross-section is the following:

$$J_i = I_i/A_i.$$

This can even be determined correctly to phase.

We mention here that with the Rogowsky coil the resultant current (I) of a self-contained high cross-section conductor, similar to an end ring, can also be measured. The current density value of the i-th cross-section related to the above is the following:

$$j_i = J_i/J_K.$$

Returning to the end ring, the diagram about the radial distribution of the current density with t = constant can be plotted by taking the mean current density values $j_1, j_2, \ldots j_n$, to the radii $r_1, r_2 \ldots r_n$ (*Fig. 4*) belonging to the centre of gravity of the partial cross-sections. As a current density of an isotropic conductor is continuous, the $j = j(r, t{=}\text{const})$ diagram can be approached with the help of a function. If we repeat this measurement and

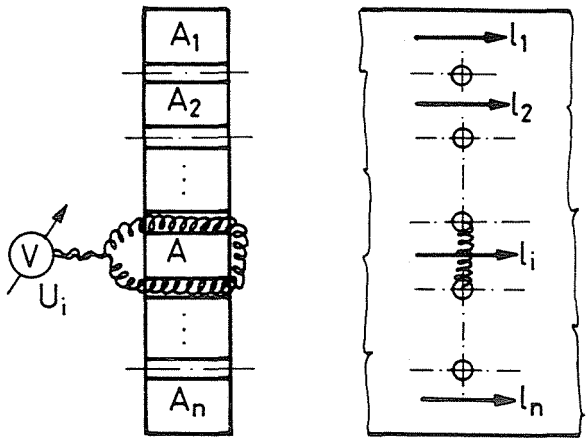

Fig. 3. Application of the Rogowsky coil for determining the current distribution on the end ring

calculation with different 't' values, a set of curves can be produced with 't' parameter. Thus, the end winding loss can be calculated in function of the distance $[p_g(t)]$ between the ring and the starting disc of a given size and material.

Fig. 5 shows a set of curves reached by measuring with t = 10, 25, 50, 75, 100 mm in the case of a rotor without starting disc ($t = \infty$). For the measurement series the end ring was divided into partial cross-sections $n = 6$ with the help of $\varnothing = 2$ mm orifices. Though the test was carried out with starting discs of different diameters and thicknesses, hereinafter we give the results achieved by a starting disc that has the diameter and thickness equal to those of the end ring.

Considering the set of curves it can be stated that the effect of starting disc on the current density distribution of the end ring is significant in the vicinity of the bar-ring connection. At this connection point — as compared to the state without starting disc — when $t = 10$ mm the current density increases in ratio 2:1. Thus, location of the starting disc near the end ring ($t < 10$ mm) is not convenient.

Fig. 6 shows the variation of the end ring loss calculated on the basis of the current density distribution set of curves in function of the 't' distance. A part $[p'_g(t)]$ of the power loss $p_g(t)$ also appears when the rotor is not provided with a starting disc. The surplus loss appearing in the ring under the effect of the starting disc is the following:

$$p''_g(t) = p_g(t) - p'_g(t).$$

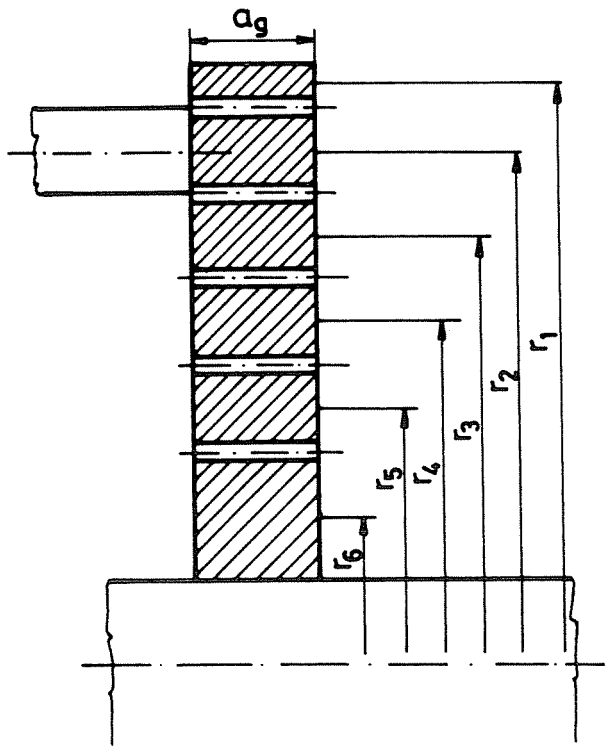

Fig. 4. Marking for the end ring dimensions

It can be read from the diagram that by the decrease of the 't' distance, not only the local loss density but also the total loss heavily increase.

2. Loss of the Starting Disc

In the course of the measurement series the star-connected stator of the end-ring model was fed by symmetric, three-phase current of constant amplitude (I_s = 80 A, f = 50 Hz). Because of the standstill condition of the rotor (short-circuited state) practically constant bar and end-ring current, — independent of the starting disc — belong to this feeding method. Correspondingly, both the stator winging loss and the loss appearing on the rotor bar section can be considered to be constant. Depending on the starting disc dimension (D_t, a_t) and on the distance from the end ring (t), the terminal voltage — necessary for maintaining the constant stator current — and the effective power input vary. The difference between the input power values measured with and without the starting disc [$\Delta P(t)$] is equal to the sum of the eddy current loss on the starting disc [$P_t(t)$] and

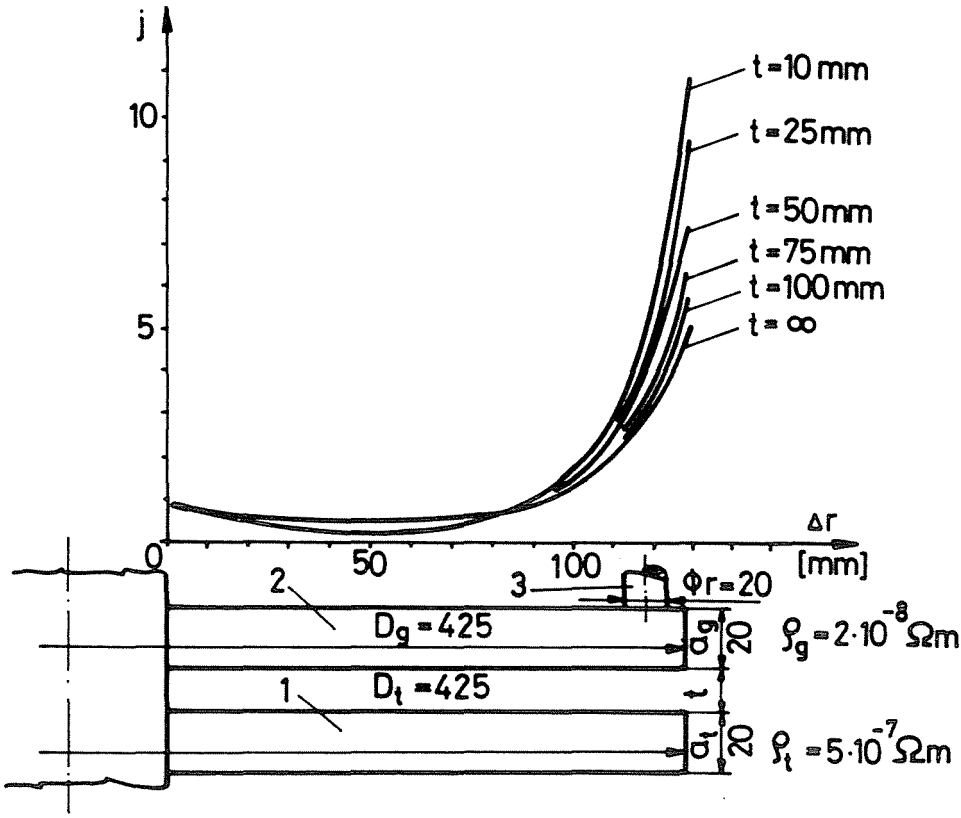

Fig. 5. Relative current density of the end ring measured along the ring height

the surplus loss of the end ring $[P_g''(t)]$. Relating this power value to the formerly introduced P_{go}:

$$\Delta p(t) = p_t(t) + p_g''(t)$$

The power loss on the rotor front side is the following:

$$p_h(t) = p_g'(t) + \Delta p(t).$$

Fig. 6 shows the $p_h(t)$ diagram as well. The intercept corresponding to the eddy current loss of the starting disc is as follows:

$$p_t(t) = p_h(t) - p_g(t).$$

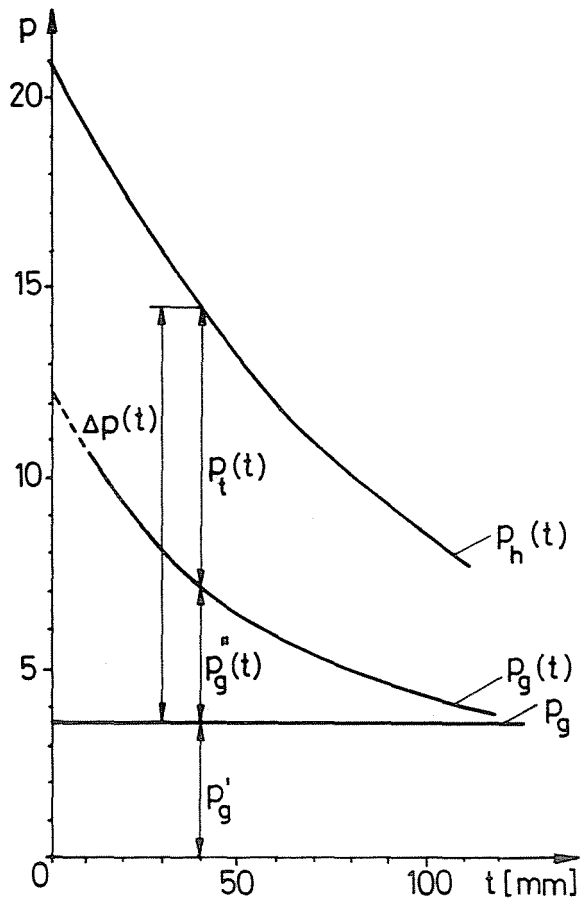

Fig. 6. Relative loss on the end ring and the starting disc, resp., in function of the distance from the disc

3. The Starting Torque

The starting torque of the induction machine can be calculated by superposing, in knowledge of the loss power components of the rotor:

$$M_i(t) = M_{ai}(t) + \Delta M_i(t).$$

Here M_{ai} means the starting torque of single-cage basic machine while $\Delta M_i(t)$ means the starting torque increase caused by the effect of the starting discs.

The starting torque of the basic machine is proportional to the P_{lt} loss, arising on the rod section of the cage winding, and the P'_g loss of the

end rings, ω_1 the synchronous angular velocity, resp.

$$M_{ai} = (P_R + P_g')/\omega_1$$

The torque component corresponding to the starting disc is as follows:

$$\Delta M_i(t) = \Delta P(t)/\omega_1 = P_{go} \cdot \Delta p(t)/\omega_1$$

The starting torque value related to the starting torque of the basic machine is the following:

$$m = 1 + \frac{\Delta M_i(t)}{M_{ai}} = 1 + \frac{P_{go}}{P_R + P_g'} \cdot \Delta p(t).$$

4. Example

Considering the shaping of the end winding space let us examine the starting torque variation for an induction machine equal to the model when distance between the ring and the starting disc varies in the range of $t = 10 \ldots 50$ mm.

On the basis of the diagram in *Fig. 6*:

$$\Delta p(t = 10 \ldots 50\,\text{mm}) = 15.7 \ldots 9.5\, p_g' = P_g'/P_{go} = 3.5.$$

The calculated value of the relative starting loss on the cage rods is:

$$P_R = P_R/P_{go} = 10.5$$

The starting torque value related to the basic machine varies in the following range:

$$m_i(t = 10 \ldots 50\,\text{mm}) = 1 + (15.7 \ldots 9.5)(10.5 + 3.5) = 2.2 \ldots 1.7.$$

Mostly, the starting torque is related to the rated M_n value. If for the real basic machine

$$M_{ai}/M_n = 0.3$$

with starting disc in the given 't' range:

$$M_i/M_n = \frac{M_{ai}}{M_n} \cdot m_i(t = 10 \ldots 50\,\text{mm}) = 0.3(2.2 \ldots 1.7) = 0.66 \ldots 0.51.$$

5. Summary

This paper describes a measurement method for the approximate determination of the current density distribution developed in the end ring of the cage type rotor. On the basis of this, the loss of the starting disc and that of the end ring, as well as the starting torque of the machine can be calculated. By examining the loss components in function of the distance between the ring and the starting disc, the expectable temperature-rise conditions of the machine parts can be estimated. The results of the measurement series highly contribute to the optimum location of the disc and to the safe machine design.

Acknowledgement

Our thanks are due to Zoltán Lengyel and Gábor Kovács for their effective help with advice and remarks.

References

1. KOVÁCS, G.: Induction Motor with a Starting Disc. *Proc. International Conference on Electrical Machines*, 1984. Lausanne, pp. 1161–1164.
2. KOVÁCS, G.: Skin Effect in the End Ring of Asynchronous Machines. *Proc. International Conference on Electrical Machines*, 1982. Budapest, pp. 31–34.
3. TRICKEY, P. H.: Induction Motor Resistance Ring Width *AIEE*, 1936, pp. 144–150.
4. WILLIAMSON, S. – BEGG, M. C. : Calculation of the Resistance of Induction Motor End Rings. *IEE Proc.* Vol. 133. Pt. B. 1986. pp. 54–60.